Latin American Journal of
Solids and Structures
www.lajss.org

Prototypes and Modulation Functions of Classical and Novel Configurations of Optical Chopper Wheels

Virgil-Florin Duma *

3OM Optomechatronics Group, Faculty of Engineering, Aurel Vlaicu University of Arad, 77 Revolutiei Ave., Arad 310130, Romania

Received 10 Jan 2012
In revised form 07 May 2012

* Author email: duma.virgil@osamember.org

Abstract

Optical choppers with rotating wheels are some of the most used macroscopic optomechatronic devices for the controlled modulation, attenuation or obscuration of light in a wide area of applications. We discuss and compare the modulation functions produced by two types of chopper wheels: the classical device, with windows with linear edges, and the eclipse chopper (with windows with circular edges) that, to the best of our knowledge, we have introduced. This discussion is based on the analysis and the design we have previously developed for these various devices, for top-hat (constant over the entire section) light beam distributions. While the comparison of the different shapes of transmitted signals allows for the proper choice of the most appropriate device and parameters to obtain the modulation function that is fit for a certain application, the present work also presents the mechanical setup we have designed and manufactured for testing choppers with rotating wheels. A series of prototype wheels with different, optimized profiles were obtained for the purpose. The simulation and the electro-erosion programs for the wire electro-erosion of aluminum plates to manufacture the wheels are presented. An advantageous double wheel solution has been developed to obtain wheels with windows of different shapes and sizes, and the testing of this final assembly concludes the study.

Keywords

optomechatronics, optical devices, choppers, modulation functions, modeling, simulations, mechanical design, prototypes, manufacturing, electro-erosion process.

1 INTRODUCTION

Choppers [2] are optomechatronic devices used for the controlled modulation or attenuation of light – especially for laser radiation. A wide range of applications benefits from them, as in telescopes and lidars [5, 21], radiometers and pyrometers [17-20], colorimeters [25], lasers [4, 24], spectral [1, 16, 28] and biomedical [8, 22, 23] systems.

Numerous studies, including early ones [6, 15, 26] approached different configurations of both macroscopic [9, 11-14] and micro- choppers [7, 27]; the latter, constructed as MEMS (Micro-Electro-Mechanical Systems) have been developed to increase the frequency of the transmitted signal above the 10 kHz limit that characterizes the macroscopic devices.

Despite the myriad of applications and the large gamut of studies, a systematic analysis and design that may cover all the possible configurations and functioning cases of choppers has not yet been achieved. We have obtained analytically the modulation functions and have developed the designing calculus of all the possible cases of the established configuration of chopper wheels, with windows with linear edges (Fig. 1a, b, Table 1) [9], for top-hat (constant over the entire section) light beam distribution. A partial experimental confirmation of our studies was made by another group for this type of wheel, for one of the cases of its working regime, when generating approximate trapezoidal output signals [3].

Another direction of research in that concerns choppers refers to other, less conventional geometrical configurations of devices, such as other types of wheels. We have introduced in this respect a new type of chopper wheel, with windows with circular edges (placed outward - Fig. 1c, or inward – Fig. 1d, Table 1) [11, 13], and we have demonstrated that it allows for producing modulation functions that are different from those that may be obtained with the classical wheels. A comparative look with regard to the classical configuration will be made in this paper, thus achieving a synthesis of our previous studies. The scope of this discussion on the different shapes of transmitted signals produced by various types of choppers is to provide rules-of-thumb to choose the most appropriate device and its characteristic parameters to obtain the modulation functions that are necessary for a certain application.

The present work also presents the mechanical setup we have designed and manufactured for testing choppers with rotating wheels both to advance our studies (especially towards other laser beams distributions, such as Gaussian and Bessel-type), and to make it available to those who carry on studies regarding these most used optomechatronic devices. Four types of prototype wheels with different, optimized profiles that we have designed and made are presented. The manufacturing trajectory of the prototypes, including the simulation and the electro-erosion programs for the wire electro-erosion of aluminum plates to obtain the wheels is provided. A double wheel solution will be developed to obtain wheels with windows of different shapes and sizes. Its testing in the final assembly will finalize the present study.

After this introduction, in Section 2 we discuss the modulation functions in relationship with specific designs of the wheels. In Section 3 we describe the characteristics of the prototype wheels (including the new types we have introduced), their manufacturing itinerary, and the modeling of the wire electro-erosion process. In Section 4 the description of the experimental module and its testing completes this work.

2 CLASSICAL AND ECLIPSE CHOPPERS: MODULATION FUNCTIONS

2.1 Geometric characteristics of the wheels

In Fig. 1 (Table 1) the configurations of chopper wheels we will discuss are presented: the first two (Fig. 1a, b) are established geometrical configurations, with windows with linear edges [9, 12], while the last two that have windows with circular edges (Fig. 1c, d) are, to the best of our knowledge, of our proposal [11, 13].

From the geometric characteristics of the wheels (Table 1) one may see that the classical chopper (Fig. 1a) is actually the particular case of the new chopper (Fig. 1c, d), obtained when

$\varrho \to \infty$. Therefore this general case, of choppers with circular-shaped edges will allow for obtaining the most general expressions of the modulation functions.

Another particular case, of the wheel in Fig. 1c, of special interest from a practical point of view is the chopper with circular windows, which is obtained for the particular case of $\alpha=0$. *As choppers are a very common device, it is essential for the profile of the windows of the wheels to be easy to be obtained with high precision and to be low cost devices.* This solution of circular windows is in this respect one that is as feasible as the one with linear edges, so by using this design one may obtain a wheel that is commercially competitive with the classical one, but it also provides other types of modulation functions, as it will be discussed further on. For experimental purposes the prototypes of the choppers with outward circular-shaped edges (Fig. 1c) will be made in this study with four windows with the angle of the window equal to the angle of the wing (opaque portion) in order to obtain a wheel with circular windows by rotating in a convenient way two identical wheels as presented in Fig. 1c in the chopper module assembly (as it will be described in Section 4).

Table 1 Parameters of the four types of prototype chopper wheels

<table>
<tr><td rowspan="3"></td><td colspan="4">Type of chopper wheels</td></tr>
<tr><td colspan="2">With windows with linear edges</td><td colspan="2">With windows with semi-circular edges</td></tr>
<tr><td>(a) ten windows</td><td>(b) two windows</td><td>(c) outward edges</td><td>(d) inward edges</td></tr>
<tr><td>Figure 1
Geometric characteristics of the chopper wheels.</td>
<td>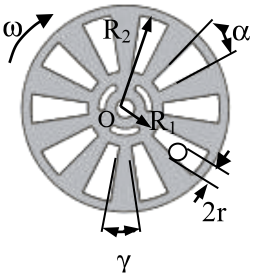</td>
<td>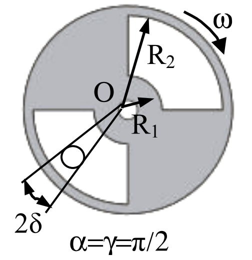</td>
<td>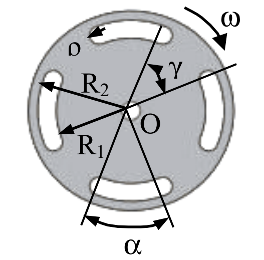</td>
<td>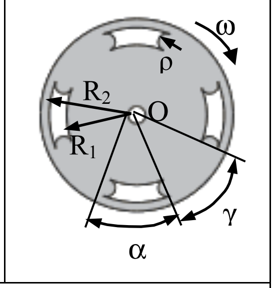</td></tr>
<tr><td>Geometric and kinematic parameters - common to all types of wheels</td><td colspan="4">n, number of wings (or of windows) of the wheel;
R_1 and R_2, minimum and maximum radius of the window, respectively;
α, angle of the window;
γ, angle of the wing (the opaque portion of the wheel) without its circular margins;
General relationship: $\alpha + \gamma = 2\pi/n$; general configuration: $\alpha \neq \gamma$;
$2r$, diameter of the light beam in the plane of the wheel;
2δ, angle of the section of the beam - as seen from the pivot O of the wheel;
ω is the constant rotational speed of the chopper wheel.</td></tr>
<tr><td>Specific geometrical parameters</td><td colspan="2">Particular (adopted) configuration: $\alpha = \gamma$ (for n=10, Fig. 1a => α = 18 degrees).</td><td colspan="2">$\varrho = (R_2\text{-}R_1)/2$, radius of the circular margins (usual functioning condition: $r < \varrho$).</td></tr>
</table>

2.2 Modulation functions of the classical choppers: with windows with linear edges

For the classical choppers wheels, with windows with linear edges (Fig. 1a, b), the modulation function of the device, which is defined by the profile of the transmitted flux, $\Phi(t)$ has to be studied with regard to the relationship between the diameter $2r$ of the section of the beam in the plane of the wheel (as seen from the pivot O, with the angle 2δ), and the angles a of the window and γ of the wing. The functions $\Phi(t)$ were obtained analytically and studied in [9] for all the possible cases of these relationships, for top-hat (with constant intensity distribution) light beams.

A synthesis of this analysis is presented bellow and (in part) in Fig. 2, where Φ_S is the incident flux (of the light source), τ_t is the transition time interval (for which the section of the beam in the plane of the wheel is progressively covered by the wing – the opaque portion of the wheel), τ is total transmission time interval, and $T=2\pi/\omega$ is the rotating period of the wheel:

(i) **Rectangular signals** are obtained when the beam is focused in the plane of the wheel (therefore the radius of the beam in this plane may be considered infinitely small for $\delta << \gamma$), and thus the obscuration time interval may be neglected ($\tau_t \approx 0$ in Fig. 2a);

(ii)**Approximate trapezoidal profiles of the signal**, Eq. (18) [9] are obtained when the above approximation cannot be used, for a finite diameter beam section in the chopper plane, and for chopper wings larger than the section of the beam ($\gamma \geq 2\delta$), for which the section can therefore be completely obscured (Fig. 2a). The characteristic time intervals of the modulation function are [9, 12]: $t_0 = (\gamma\text{-}2\delta)/\omega$; $\tau_t = 2\delta/\omega$; $\tau = ((a\text{-}2\delta)/\omega$. Our theoretical findings were in part confirmed experimentally for this trapezoidal profile by another group [3];

(iii) **Approximate sinusoidal signals** (but with the more complicated equation studied in [9] – Eq. (18)) are obtained for the particular case $a = 2\gamma = \delta$;

(iv) **Non-null signals** (Fig. 2b) when the chopper has a single narrow wing in the section of the beam (for $\gamma < 2\delta$ and $a > 2\delta + \gamma$) – Fig. 2b Eq. (29) [9] (where Φ_{min} is reached when the wing is situated symmetric, in the center of the section, Eq. (30) [9]); $M = \Phi_S / \pi r^2$ is the brightness of the input signal, constant over the entire beam section (the definition of top-hat light beams);

(v) **Approximate sinusoidal non-null signals** (for which an example is shown in Fig. 2c), for wheels with several wings in front of the beam section (for a, $\gamma < 2\delta$, where there are two cases, for $a < \delta + \gamma/2$ (the case in Fig. 2c), and for $\delta + \gamma/2 < a < 2\delta$, the latter with a similar profile, but with a smaller possible amplitude. The obscuration area A studied for a wing that rotates in front of the section in case (iv) allowed for obtaining the SA function in this case (for multiple wings in front of the section), which provides the flux function $\Phi(t)$ - Eq. (32) [9].

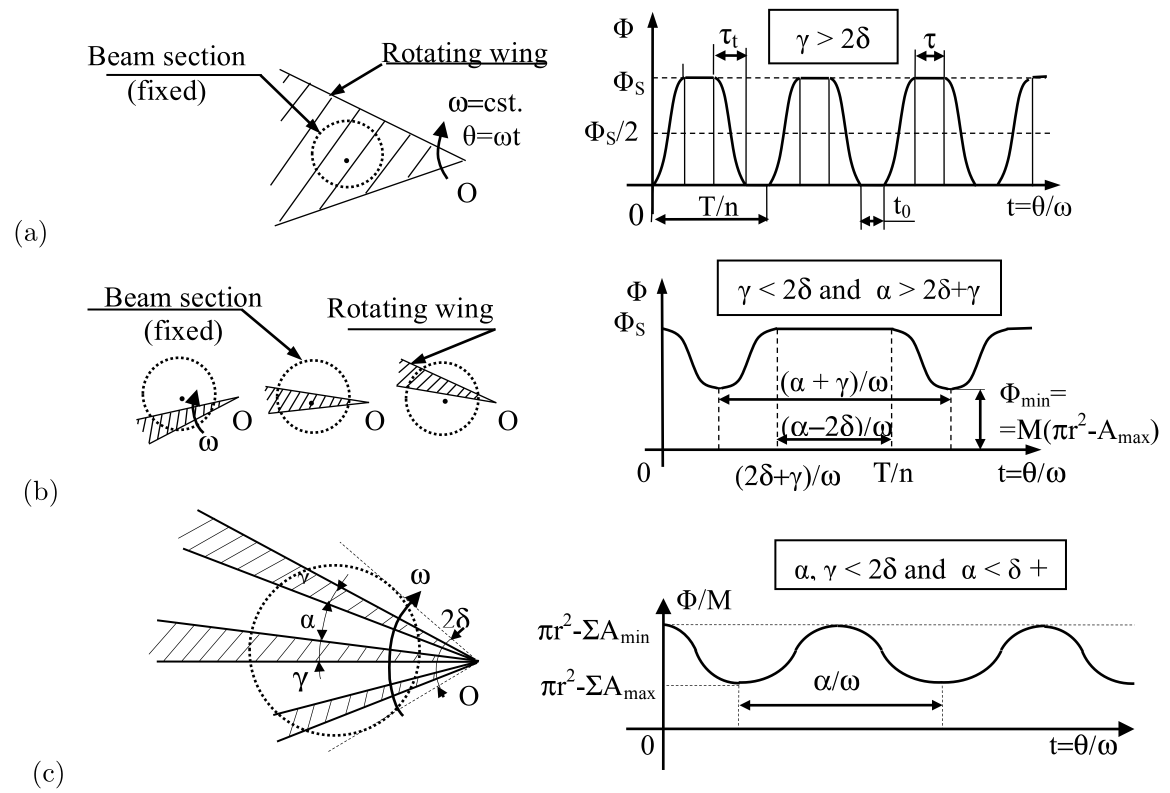

Figure 2 Chopper wheels (classical configurations, with windows with linear edges): Transmission (modulation) functions produced for beams with finite diameters, and for: (a) wings of large angles (γ); (b) wings of small angles, with only one wing at a time in the beam section; (c) the general case of multiple narrow wings in the section of the light beam

2.3 Modulation functions of the eclipse choppers

Choppers with curved, in particular circular edges of the windows, both outward (Fig. 1b) and inward (Fig. 1c) were introduced [11, 12] and studied [12-14] with regard to their transmission functions. We have named this new configuration, due to the fact that the obscuration process of the beam section by the circular margin is similar to a planetary eclipse (Fig. 3a), **the "eclipse" chopper**. As pointed out in Section 2 a most practical configuration of this chopper with outward margins is the one when the two edges merge, producing a wheel with circular holes – solution actually considered in Fig. 3a.

The functions of the transition phases are similar for the outwards and inwards margins (Fig. 6b), although the time intervals are different for the same values of a and γ due to the orientation of the window edges [13, 14]. This gives an overall higher transmission coefficient for the device with outward margins, even if (as shown in Fig. 3d) the device with inward margins gives a slightly higher transmission flux for the transition period.

From the equations of the transmission functions of these choppers (i.e. Eqs. (9) and (10), Table 1) [9, 13], an interesting result was reached: **approximate triangular signals** can be obtained with this type of wheels for $a \pm 2(\varphi \mp \delta) = 0$ (from Fig. 3b, for outward, respectively inward edges), as seen in Fig. 3c where the margins (the transition phases) of the transmitted signal were represented for the numerical example considered; the unitless *flux factor* $f(t)=\Phi(t)/M\pi r^2$ (M, brightness) has been considered in these graphs to make the representation more convenient. This is in contrast to classical choppers, which can only provide, for such a condition, approximate sinusoidal signals – case (iii), Section 2.2. Of course, when $\varrho\to\infty$ in the configuration of the eclipse chopper wheel, the triangular signal shifts into the sinusoidal one.

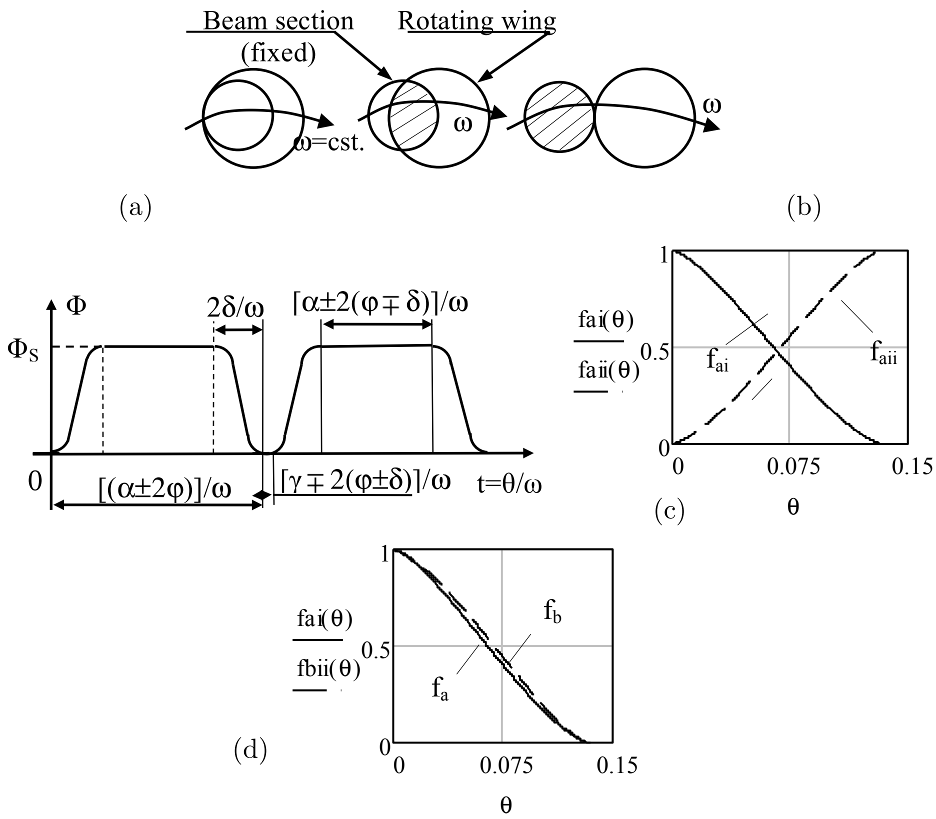

Figure 3 Chopper with outward edges: (a) obscuration of the section of the beam; (b) Modulation functions, for outward, respectively inward edges; (c) *Flux factor* $f(t)=\Phi(t)/M\pi r^2$ (M, brightness) in the transition periods (f_{ai} for the obscuration and f_{aii} for the unobscuration of the beam) for R=60 mm, ρ=20 mm, r=4 mm; (d) comparison between the flux factor for outward (f_a) and for inward (f_b) edges

3 PROTOTYPE CHOPPER WHEELS

In order to carry on multi-parametric analyses of the modulation functions produced by each type of wheels, without having to manufacture a different wheel, with different geometrical parameters (i.e., angles α and γ – Table 1), the chopper module we have designed has a pair of identical wheels at a time, one fix and the other one with adjustable (rotational) position in the assembling phase. Thus, the window angle can be adjusted in a certain range (equal to the angle α) prior to starting the device, to allow for generating light impulses with different durations – for the same range of the rotation speed ω.

3.1 Manufacturing itinerary of the chopper wheels

Two examples of chopper wheels blueprints are shown in Fig. 4: (a) with ten windows (Fig. 1a); (b) with four windows, with outward circular margins (Fig. 1c). These specific wheels have been considered for the chopper prototypes as they are the most used (and useful) for the optics community.

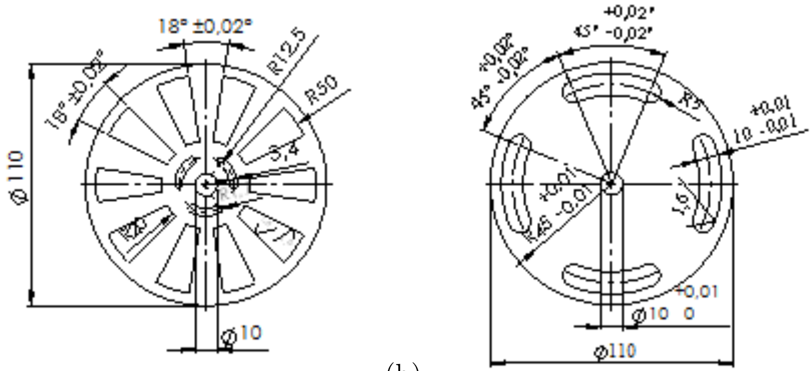

(a) (b)

Figure 4 Blueprints of two chopper wheels (with the dimensions provided in mm): (a) with ten windows and linear edges; (b) with four windows and outward circular edges

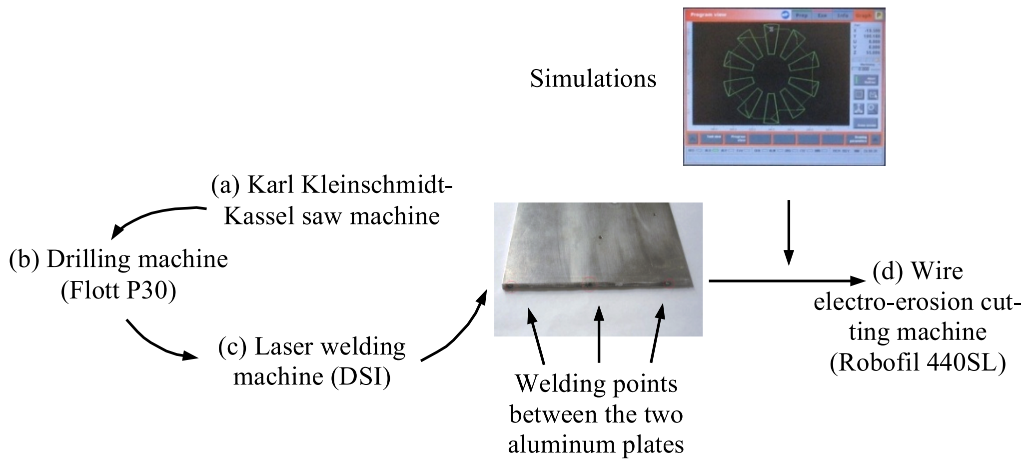

Figure 5 Trajectory of the manufacturing process of the prototype chopper wheels

In Fig. 5 the manufacturing process of the prototypes is described, in its essential steps, with the machines used pointed out: (a) *cutting the plates* (from an aluminum sheet of thickness 3 mm at 150 x 150 mm); (b1) *drilling – phase 1* (the holes for the wire are positioned first, a circle is divided in n equal parts at $\alpha + \gamma$, the n intersections and the centre of the future disc are marked manually, and in all these points Ø1.5 mm diameter holes are done); (c) *welding two plates* together with a laser system (to obtain the two necessary identical wheels at a time – as explained above); (b2) *drilling – phase 2* (Ø3 mm holes are done to allow, in the electro-erosion process that follows, the wire to pass to the next phase); (d) *wire electro-erosion* of the windows and of the disc - after completing the simulations of this process for each type of wheel.

3.2 Simulations and the electro-erosion process

The simulations for the electro-erosion process are presented, for each of the four types of windows, in Fig. 6. The programs of the process are (Table 2): (i) the command program O1 selects the parameters of the process with regard to the material of the piece (aluminum, in this case), the diameter of the wire, the rough and the finishing regime; (ii) the program O2000 generates the profile of each of the four types of wheels; (iii) the cycle O1000 is followed for each wheel to pass from one window to another and thus to complete the process.

In Fig. 7 two steps of the electro-erosion process are shown for each chopper wheel.

Table 2 The electro-erosions programs of the four prototype wheels

<table>
<tr><td colspan="3">Command Program O1.iso</td></tr>
<tr><td colspan="2">N10 G11 WIR , LS 25
N20 G11 TEC , O1
N30 M31
N40 G10 P16 R ,0
N50 G92 X0. Z0. H6.
N60 G10 P0 B0
N70 G10 P1 B1
N80 S501
N90 M98 P1000 Q0
N100 G10 P0 B1
N110 G10 P1 B0
N120 S502
N130 M98 P1000 Q0
N140 G90
N150 G10 P0 B0
N160 M30</td><td>Significance of the functions in the program O1:
G11 WIR – Activation of wire table; G11 TEC – Activation of Technology table; M31 – Setting of machining counter to zero; G10 R – Modify the User parameters CLE or Rmin. Enable/Disable optional block skip; S501 - Selection of a setting of the Sequence; M98 P – Sub-program call; S502 – Finishing regime; G90 – Absolute mode-Part coordinates; M30 – End of program or sub-program and re-reeling.</td></tr>
<tr><td colspan="3">Program O2000 to generate the profile</td></tr>
<tr><td colspan="2">For the wheel with linear edges of the windows</td><td>For the wheel with circular edges of the 4 windows</td></tr>
<tr><td>(a) with 10 equidistant windows (Figs. 1a, 6a)</td><td>(b) with 2 windows (Figs. 1b, 6b)</td><td>(c) with outward edges (Figs. 1c, 6c)</td></tr>
</table>

Table 2 continued

<table>
<tr>
<td>M29
G92 X0 Y45.
N10 G41 G01 X-7.821 Y49.384
N20 G01 X-3.128 Y19.753
N30 G02 X3.128 I3.128 J-20.
N40 G01 X7.821 Y49.384
N50 G03 X-7.821 I-7.821 J-50.
N60 G40 G01 X0. Y45.
N70 M50
N80 G00 X-26.45 Y36.405
N90 M60
N100 M30</td>
<td>M 29
G92 X5. Y23.
N10 G41 G01 X0. Y18.
N20 G02 X18. Y0. I0. J-18.
N30 G01 X50.
N40 G03 X0. Y50. I-50. J0.
N50 G01 Y18.
N60 M00
N70 G40 G01 X5. Y23.
N80 M30</td>
<td>G75 X-17.221 Y41.575
M29
G92 X-17.221 Y41.575
N10 G01 G42 X-19.134 Y46.194
N20 G02 X19.134 Y46.194 I19.134 J-46.194
N30 G02 X22.221 Y 41.575 I-1.913 J-4.619
N40 G02 X17.221 Y36.575 I-5. J 0.
N50 G02 X15.307 Y36.955 I0. J5.
N60 G03 X-15.307 Y36.955 I-15.307 J-36.955
N70 G02 X-17.221 Y36.575 I-1.91 J4.62
N80 G02 X-22.221 Y41.575 I0. J5.
N90 G02 X-17.221 Y46.575 I5. J0.
N100 M00
N110 G01 G40 X-17.221 Y41.575
N120 M30</td>
</tr>
<tr>
<td colspan="3">Significance of the functions in the program O2000 above:
M29 – Second level roughing protection strategy on; G75 – Positioning in the Machine coordinate system; G92 – Definition of the Part system of coordinates; G41 – Offset to left; G01 – Linear interpolation; G02 – Circular interpolation (clockwise processing speed); G03 – Circular interpolation (counter clockwise processing speed); M00 – Program stop; G40 – Cancelling of offset; M50 – Wire cut; G00 – Rapid traverse; M60 – Wire threading.</td>
</tr>
<tr>
<td colspan="2">Cycle O1000 – the program above is repeated in this routine to obtain the multiple windows
G90
N10 G92 X0. Y45.
N20 M98 P2000 Q36. L10.
N30 M30</td>
<td>Significance of the functions in the Cycle O1000: G90 – Absolute mode-Part coordinates; G92 – Definition of the Part system of coordinates; M98 – Sub-program call; P2000 – Name of the subroutine; Q36 – Rotation angle; L10 – Repetition number.</td>
</tr>
</table>

(1)

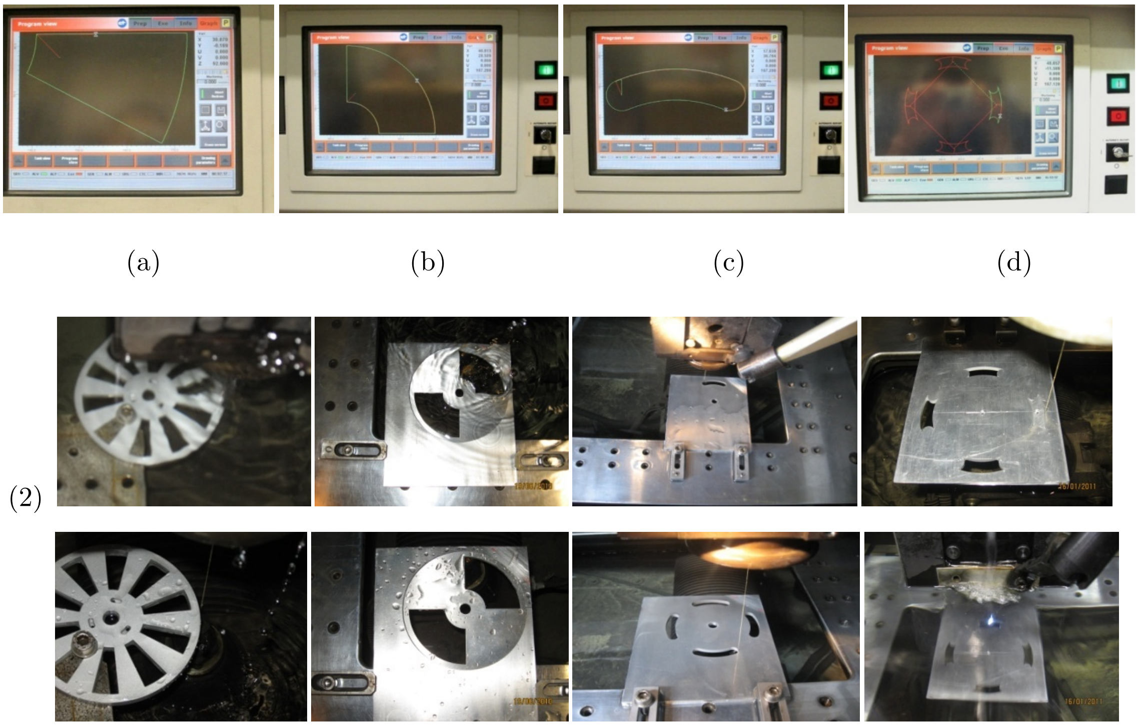

(a) (b) (c) (d)

(2)

(a) (b) (c) (d)

Figure 6 Wire electro-erosion of the four types of chopper wheels: for the classical chopper (a) with ten, and (b) with two windows with linear margins; for the eclipse chopper, with windows with (c) outward, and (d) with inward circular edges. Phases: (1) Simulations for the electro-erosion of a window; (2) manufacturing of a wheel - for each type of chopper

4 EXPERIMENTAL SETUP AND TESTS

In Fig. 7 the principle of the experimental stall we have designed for the study of chopper wheels (including those in Fig. 1) is presented. The laser source (He-Ne diode with the wavelength λ equals 670 nm and an output power of 5 mW) generates a beam that is chopped by a rotating wheel, driven by a motor (power 300 W) equipped with a potentiometer for adjusting its rotational speed ω. A photo-diode receives the output signal of the chopper and the modulation functions produced are recorded by an oscilloscope (RIGOL 5202 MA) that also sends the data to a PC.

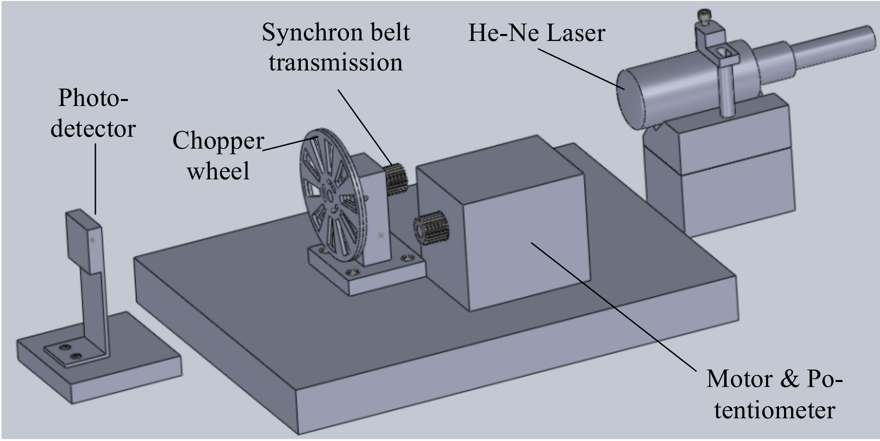

Figure 7 Experimental setup developed for the study of choppers – principle scheme

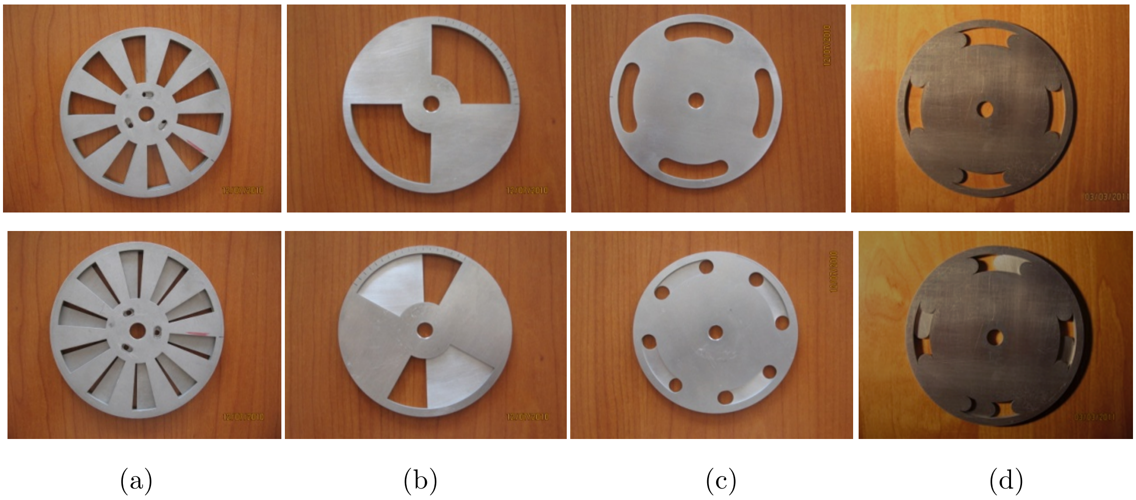

Figure 8 Different positions of the pairs of two identical wheels for each of the four prototypes to obtain different window angles of the chopper module in the final assembly: (a) with ten, and (b) with two windows with linear margins; with windows with (c) outward, and (d) with inward circular margins.

Figure 8 shows the four types of wheels manufactured. For each type, two identical pieces were obtained (as pointed out in Section 3). In Figs. 8 and 9 these two identical wheels (marked in degrees on the lateral margins) are assembled to form a wheel, therefore an adjustable windows with the desired angle is obtained prior to starting the device. The chopper will thus have a window angle α that can be varied from 0 to the constructive angle α of a single wheel. In Fig. 8c, the particular α=γ configuration choosed allows for obtaining, with this pair of identical wheels, a chopper with 8 circular holes, due to the superposition of the 4 windows - when two circular outward margins are bounded together to form a 2ϱ diameter window (thus α=0).

Figure 9a shows the constructive solution of the chopper module with the 10 windows wheel mounted on it, and Fig. 9b and c the assembled module with two different types of wheels.

In Fig. 10 the results of the testing of the experimental module are presented, for two cases that are specific to the configuration manufactured, with the opaque portion larger than the section of the beam in the plane of the wheel (cases (i) and (ii), Section 2.2).

Figure 9 Chopper module: blueprint (a); assembly of the wheels with linear (b) and with circular outward (c) edges.

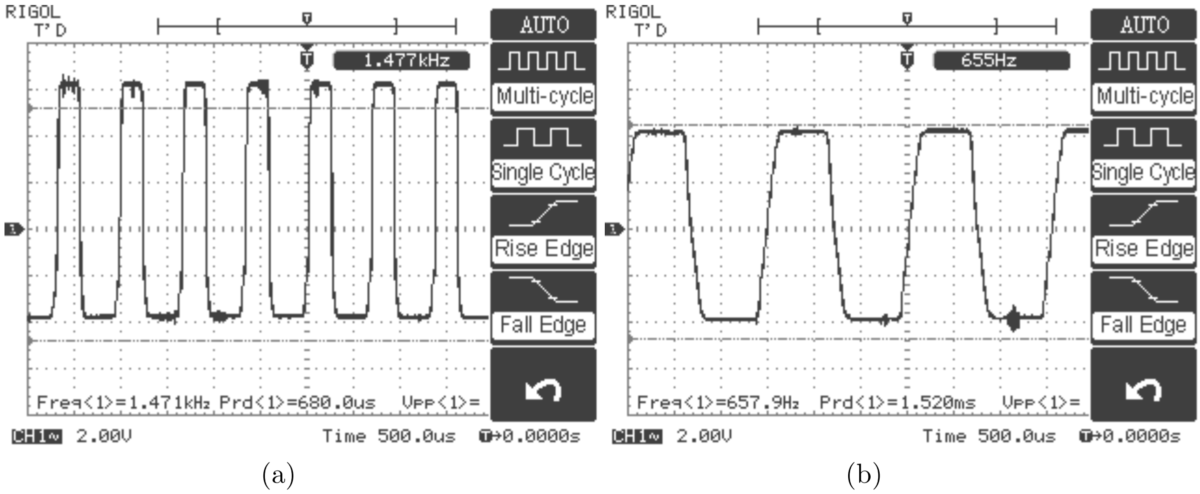

Figure 10 Test of the modulation functions for the chopper wheel with ten windows and linear edges: (a) rectangular, for the laser beam focused in the plane of the wheel; (b) trapezoidal, for a beam of finite diameter in the plane of the wheel

5 CONCLUSIONS

We have discussed the modulation functions produced by different configurations of chopper wheels, from the classical ones (with windows with linear edges) to the eclipse choppers (with circular, outward or inward edges) that, to the best of our knowledge we have introduced [13]. This discussion, which syntetized several of our previous studies [9, 12-14] allowed for extracting rules-of-thumb that are necessary to allow for choosing the proper wheel design (type and parameters) to obtain the modulation function that is required in a certain application.

We have also presented the design and manufacturing phases of four representative types of prototype wheels that we have developed, both with windows with linear and with circular edges. These wheels were monted in a double wheel assembly to allow for adjusting the window angle to obtain wheels with different parameters, and this module has been tested for wheels with large obscuration portions. This chopper module thus will be used to study further on the modulation of light produced by different configurations of wheels that are in development both in our group and in the optics community. Also, while we have obtained until now only the theory of choppers for top-hat (constant) light beam distributions, the cases of other types of beams (e.g., Gaussian, Airy and Bessel), of high interest for a variety of applications, especially for the optics and biomedical imaging community are another essential direction of research. Another aspect concerns the use of choppers as optical attenuators, in competition with other devices, such as Risley prisms [10]. These studies are in our general direction of research concerning the radiometry of optical systems [11].

Future work, both theoretical and experimental thus adresses the development (analysis, modeling, simulation, design, manufacturing and testing) of chopper wheels with profiles that may generate different, required profiles of the light flux functions transmitted. Besides this need to solve the inverse problem of these widely used optomechatronic devices, new types of choppers are required to produce signal frequencies that may go beyond the 10 kHz limit of macroscopic choppers, and that may be also subject of miniaturization as MEMS.

Acknowledgements

The paper is in part based on a presentation made at the *11th Conference on Dynamical Systems - Theory and Applications (DSTA),* Łódź, 5-8 December 2011, chaired by Prof. J. Awrejcewicz. This research is currently funded by a grant of the Romanian National Authority for Scientific Research, CNDI-UEFISCDI, project number PN-II-PT-PCCA-2011-3.2-1682. As part of this work has begun in 2009-2010, the support of the US Department of State through Fulbright Scholar Grant 474/2009 is also gratefully acknowledged. Special thanks to Mihai Kiss for his invaluable help with the experimental part.

References

[1] F. Barone, U. Bernini, M. Conti, A. Del Guerra, L. Di Fiore, M. Gambaccini, R. Liuzzi, L. Milano, G. Russo, P. Russo, and M. Salvato. Detection of X rays with a fiber-optic interferometric sensor. *Applied Optics,* 32:1229-1233, 1993. http://dx.doi.org/10.1364/AO.32.001229

[2] M. Bass. *Handbook of Optics.* 2nd edition, 2001 (Mc. Graw-Hill, New York, US).

[3] K. Benjamin, A. Armitage, and R. South. Harmonic errors associated with the use of choppers in optical experiments. *Measurement,* 39:764-770, 2006. doi:10.1016/j.measurement.2006.02.008

[4] R. M. J. Benmair, J. Kagan, Y. Kalisky, Y. Noter, M. Oron, Y. Shimony, and A. Yogev. Solar-pumped Er,Tm,Ho:YAG laser. *Optics Letters*, 15:36-38, 1990 http://dx.doi.org/10.1364/OL.15.000036

[5] H. Bittner, M. Erdmann, B. Herdt, and A. Steinacher. Optical system of the SOFIA Telescope. *Proc. SPIE,* 3356:512-521, 1998. http://dx.doi.org/10.1117/12.324474

[6] J. L. Bufton, S. C. Cohen. Fourier Spectrum of a Chopped Bivariate Normal Intensity Distribution. *Applied Optics*, 9:381-384, 1970. http://dx.doi.org/10.1364/AO.9.000381

[7] M. T. Ching, R. A. Brennen, and R. M. White. Microfabricated optical chopper. *Optical Engineering.* 33:3634-3642, 1994. http://dx.doi.org/10.1117/12.181576

[8] R. G. Cucu, A. Gh. Podoleanu, J. A. Rogers, J. Pedro, and R. B. Rosen. Combined confocal/en face T-scan-based ultrahigh-resolution optical coherence tomography in vivo retinal imaging. *Optics Letters,* 31:1684-1686, 2006. http://dx.doi.org/10.1364/OL.31.001684

[9] V. F. Duma. Theoretical approach on optical choppers for top-hat light beam distributions. *Journal of Optics A: Pure and Applied Optics,* 10:064008, 2008. http://iopscience.iop.org/1464-4258/10/6/064008/

[10] V. F. Duma and M. Nicolov. Neutral density filters with Risley prisms: analysis and design. *Applied Optics,* 48:2678-2685, 2009. http://dx.doi.org/doi:10.1364/AO.48.002678

[11] V. F. Duma. Radiometric versus geometric, linear and non-linear vignetting coefficient. *Applied Optics,* 48(32):6355-6364, 2009. http://dx.doi.org/10.1364/AO.48.006355

[12] V. F. Duma, M. Nicolov, and M. Kiss. Optical choppers: modulators and attenuators. *Proc. SPIE*, 7469:74690V, 2010. http://dx.doi.org/10.1117/12.859044

[13] V. F. Duma. Optical choppers with circular-shaped windows: Modulation functions, *Communications in Nonlinear Science and Numerical Simulation,* 16(5):2218-2224, 2011. http://dx.doi.org/10.1016/j.cnsns.2010.04.043

[14] V. F. Duma. Optical choppers with rotating wheels: Classical and novel configurations, and their modulation functions. *Dynamical Systems. Nonlinear Dynamics and Control*, Awrejcewicz J., Kazmierczak M., Olejnik, P., Mrozowski J., Eds., Łódź, 2011, pp. 109-114.

[15] T. E. Furtak. Sinusoidal radiation chopper for modulation of the maximum available light intensity. *Applied Optics,* 16:803-804, 1977. http://www.opticsinfobase.org/ao/abstract.cfm?URI=ao-16-4-803

[16] M. A. Gondal and Z. H. Yamani. M. A. Gondal and Z. H. Yamani. Highly sensitive electronically modulated photoacoustic spectrometer for ozone detection. Applied Optics, 46:7083-7090, 2007. http://dx.doi.org/10.1364/AO.46.007083

[17] Y. He, W. Jin, G. Liu, Z. Gao, X. Wang, and L. Wang. Modulate chopper technique used in pyroelectric uncooled focal plane thermal imager. *Proc. SPIE*, 4919:283-288, 2002. http://dx.doi.org/10.1117/12.471869

[18] Koepernik J., Budzier H., Hofmann G.: Influence of nonideal chopper design on nonuniformity in uncooled pyroelectric staring array systems. *Proc. SPIE* 2552:624-635, 1995. http://dx.doi.org/10.1117/12.218261

[19] V. N. Leonov and D. P. Butler. Two-color Thermal Detector with Thermal Chopping for Infrared Focal-Plane Arrays. *Applied Optics*, 40:2601-2610, 2001. http://dx.doi.org/10.1364/AO.40.002601

[20] A. Makoui and D. K. Killinger. Transient fluorescence spectroscopy of terbium doped dipicolinic acid: a fluorescence lifetime measurement technique. *JOSA B*, 26:691-698, 2009. http://dx.doi.org/10.1364/JOSAB.26.000691

[21] I. S. McDermid, G. Beyerle, D. A. Haner, and T. Leblanc. Redesign and improved performance of the tropospheric ozone lidar at the jet propulsion laboratory table mountain facility. *Applied Optics,* 41:7550-7555, 2002. http://dx.doi.org/10.1364/AO.41.007550

[22] H. Olkkonen. Chopper stabilized laser-Doppler skin blood velocimeter. *Proc. SPIE,* 1922:219-224, 1993. http://dx.doi.org/10.1117/12.146203

[23] A. Gh. Podoleanu, G. M. Dobre, and R. G. Cucu. Sequential optical coherence tomography and confocal imaging. *Optics Letters,* 29:364-366, 2004. http://dx.doi.org/10.1364/OL.29.000364

[24] R. Scheps and J. F. Myers. Performance of a diode-pumped laser repetitively Q-switched with a mechanical shutter. *Applied Optics,* 33:969-978, 1994. http://www.opticsinfobase.org/ao/abstract.cfm?URI=ao-33-6-969

[25] W. Small, P. M. Celliers, L. B. Da Silva, D. L. Matthews, and B. A. Soltz. Two-Color Mid-Infrared Thermometer With a Hollow Glass Optical Fiber. *Applied Optics,* 37:6677-6683, 1998. http://dx.doi.org/10.1364/AO.37.006677

[26] D. Vincent. Amplitude modulation with a mechanical chopper. *Applied Optics,* 25:1035-1036, 1986. http://dx.doi.org/10.1364/AO.25.001035

[27] M. Ueda, T. Shiono, T. Ito, and K. Yokoyama. High-efficiency diffractive micromachined chopper for infrared wavelength and its application to a pyroelectric infrared sensor. *Applied Optics,* 37:1165-1170, 1998. http://dx.doi.org/10.1364/AO.37.001165

[28] K. Wang and L. Zeng. Two-dimensional surface profile imaging technique based on a double-grating frequency shifter. *Applied Optics,* 44:4625-4630, 2005. http://dx.doi.org/10.1364/AO.44.004625